

RESEARCH ARTICLE

10.1002/2017JA024265

Key Points:

- The equatorial ionosphere response to different disturbed electric fields is analyzed using the SUPIM-INPE model
- We want to find the best alternative of disturbed electric field, both temporally and spatially, when $\mathbf{E} \times \mathbf{B}$ measurements are not available
- The comparison between simulations and observations will serve to find a hierarchy among the different types of drifts

Supporting Information:

- Supporting Information S1

Correspondence to:

M. A. Bravo,
manuel.bravo.s@usach.cl

Citation:

Bravo, M. A., Batista, I. S., Souza, J. R., & Foppiano, A. J. (2017). Equatorial ionospheric response to different estimated disturbed electric fields as investigated using Sheffield University Plasmasphere Ionosphere Model at INPE. *Journal of Geophysical Research: Space Physics*, 122, 10,511–10,527. <https://doi.org/10.1002/2017JA024265>

Received 17 APR 2017

Accepted 12 SEP 2017

Accepted article online 14 SEP 2017

Published online 13 OCT 2017

Equatorial Ionospheric Response to Different Estimated Disturbed Electric Fields as Investigated Using Sheffield University Plasmasphere Ionosphere Model at INPE

M. A. Bravo^{1,2} , I. S. Batista¹ , J. R. Souza¹, and A. J. Foppiano³ 

¹Instituto Nacional de Pesquisas Espaciais, São José dos Campos, São Paulo, Brazil, ²Now at Universidad de Santiago de Chile, Estación Central, Santiago, Chile, ³Universidad de Concepción, Concepción, Chile

Abstract Good ionospheric modeling is important to understand anomalous effects, mainly during geomagnetic storm events. Ionospheric electric fields, thermospheric winds, and neutral composition are affected at different degrees, depending on the intensity of the magnetic disturbance which, in turns, affects the electron density distribution at all latitudes. The most important disturbed parameter for the equatorial ionosphere is the electric field, which is responsible for the equatorial ionization anomaly. Here various electric field measurements and models are analyzed: (1) measured by the Jicamarca incoherent scatter radar (ISR), (2) from Jicamarca Unattended Long-Term studies of the Ionosphere and Atmosphere (JULIA) radar, (3) deduced from magnetometers, (4) calculated from the time variations of the F layer height (dh'/dt), and (5) deduced from interplanetary electric field determinations. The response of ionospheric parameters f_oF_2 and h_mF_2 to the electric fields simulated using the Sheffield University Plasmasphere Ionosphere Model version available at Instituto Nacional de Pesquisas Espaciais is compared with observations for two locations, during the geomagnetic storm events of 17–18 April 2002 and 7–10 November 2004. Results are found to be consistent with the observations in such a way that a hierarchy among the different types of drifts used can be established. When no ISR measurements are available, the drifts deduced from magnetometers or measured by the JULIA are best when including the contribution derived from dh'/dt for the 18–24 LT time interval. However, when none of these drifts are available, drifts inferred from the interplanetary electric field seem to be a good alternative for some purposes.

1. Introduction

Solar events generate geomagnetic disturbances on Earth, and big changes in the electrical current system, circulation of winds, and composition in the upper atmosphere are produced. These changes disturb directly the global ionosphere. Historically, they have been known for long time (e.g., Rishbeth, 1975; Prolss, 1977, among many others). The equatorial and low-latitude ionosphere are affected mainly by ionospheric zonal electric field disturbances (Abdu, 2005; Kelley, 2009), the middle latitudes are by disturbed neutral wind (Rishbeth, 1975), and the high latitude by changes in the chemical composition of the atmosphere driven by Joule heating (Prolss & von Zahn, 1974; Tausch, Carignan, & Reber, 1971; Torres Pincheira, 1998).

During a geomagnetic storm, the ionospheric zonal electric field can be affected in two ways: due to the prompt penetration electric fields (PPEFs) from the magnetosphere and, subsequently, due to the disturbance dynamo (DD) (Blanc & Richmond, 1980). The PPEFs are directly related to changes in the B_z component of the interplanetary magnetic field ($\text{IEF} = -V_{\text{SW}} \times B_z$, where IEF is the interplanetary electric field and V_{SW} is the solar wind velocity). In particular, when B_z turns southward (undershielding) the PPEF and quiet time atmospheric dynamo electric field are in phase, and when B_z turns northward (overshielding) the PPEF is in opposite phase to the quiet time atmospheric dynamo electric field (Kelley, 2009; Wolf et al., 2013). These PPEFs occur, generally, in the early hours of the geomagnetic storm (in contrast to the DD), penetrating from high to low latitudes and altering significantly the vertical drift of the equatorial ionosphere ($\mathbf{E} \times \mathbf{B}$ drift).

Many authors used numerical models in an attempt to reproduce the observed ionospheric effects of geomagnetic storms (e.g., Balan et al., 2009, 2010, 2013; Batista et al., 1991, 2006; Fang et al., 2007; Fuller-Rowell et al., 1996, 2007; Joshi et al., 2016; Lin et al., 2005; Lin, Richmond, Liu, et al., 2009; Lin, Richmond, Bailey, et al., 2009; Lu et al., 2012; Maruyama et al., 2005, 2007; Pincheira et al., 2002; Retterer & Kelley, 2010; Richmond et al., 2003, among others). Specifically, if we want to mainly model

the storm equatorial ionosphere dynamics, we must modify its quiet zonal electric field input. Such parameter, for example, is more efficient to control the equatorial F layer height motion than the thermospheric neutral wind.

A problem for modeling disturbed periods is the poor availability of zonal electric field measurements, both in space and time. It is necessary to find alternatives to cover the lack of measurement. Alternative measurements and models could be the Jicamarca Unattended Long-Term studies of the Ionosphere and Atmosphere (JULIA) measurements at 150 km height (Chau & Woodman, 2004), the drift deduced from magnetometer measurements (Anderson et al., 2002, 2004) and the drift calculated from the time variations of the ionosonde determined F layer height (Bittencourt & Abdu, 1981) or from HF Doppler observations of that height (Joshi et al., 2016). All these alternatives have some time limitations. Furthermore, there is also a good correlation between the IEF and the zonal electric field measured at Jicamarca Radio Observatory. This correlation is positive during the day and negative during the night. Some authors have found that the penetration of the IEF to the equatorial ionosphere electric field has efficiencies between 3% and 14% (e.g., Burke et al., 2007; Denardini et al., 2011; Huang et al., 2007, 2010; Kelley et al., 2003; Kelley & Retterer, 2008; Retterer & Kelley, 2010; Wei et al., 2008). The advantage of this alternative is that it has a greater temporal availability.

In the present work we analyze the ionospheric response to different disturbed electric field (or $\mathbf{E} \times \mathbf{B}$ vertical drift) models, using an ionospheric model (Sheffield University Plasmasphere Ionosphere Model–Instituto Nacional de Pesquisas Espaciais (SUPIM-INPE)), to find the best disturbed electric field alternative, both temporally and spatially, when/where $\mathbf{E} \times \mathbf{B}$ vertical drift measurements are not available. The comparison between simulations and observations will serve to find a hierarchy among the different types of drifts. We believe that this work is the first comparative study of different drift models using a plasmasphere-ionosphere model. The modeling of the equatorial ionosphere during disturbed periods using the appropriate zonal electric field would help to understand the significant disturbances found in the electron density distribution: the equatorial electrojet (EEJ) and the equatorial ionization anomaly (EIA) development. Since the analyses do not relate to a given longitude sector, the results could be applied to all longitudes as a first approximation. Moreover, it would be useful for extending the modeling to low and middle latitudes.

2. Models and Data

In this work we use the Sheffield University Plasmasphere Ionosphere Model (SUPIM) (Bailey & Balan, 1996; Bailey & Sellek, 1990; Bailey, Sellek, & Rippeth, 1993) to simulate the ionospheric behavior at different stations in the equatorial regions in South America during some geomagnetically disturbed events. SUPIM has been modified by the Aeronomy Division of the Atmospheric and Space Science Coordination at Instituto Nacional de Pesquisas Espaciais (INPE) to include the E region and to update some inputs (Santos et al., 2016; Souza et al., 2010, 2013).

The SUPIM solves the coupled time-dependent equations of continuity, momentum, and energy balance for the ions (O^+ , H^+ , He^+ , N_2^+ , NO^+ , and O_2^+) and electrons along closed magnetic field lines. The SUPIM-INPE extends the calculations along the magnetic field lines from its original lower apex and base altitude limits from 150 km and 130 km (Bailey et al., 1993; Bailey & Balan, 1996) down to 90 and 80 km, respectively, and adds the calculations for a seventh ion N^+ (Souza et al., 2010, 2013). In addition, the chemical reaction scheme from Huba, Joyce, and Fedder (2000), which is prepared to include E region, has been used. The photochemical equilibrium condition was applied only at the base altitudes as also used by original SUPIM. The main input parameters to this model are the zonal electric field (or, in this case, the $\mathbf{E} \times \mathbf{B}$ vertical drift), the neutral wind, the neutral densities, and the EUV flux. The neutral winds and densities are from the horizontal wind model 1993 (HWM93) (Hedin et al., 1996) and the NRLMSISE-00 (Picone et al., 2002), respectively. The ionizing solar flux is from EUVAC (Richards et al., 1994) except for the X-ray and Lyman α fluxes which are obtained from the SOLAR2000 model (Tobiska et al., 2000).

In the case of the $\mathbf{E} \times \mathbf{B}$ vertical drift input, SUPIM-INPE uses the drifts for 2 days: the day to be simulated and the previous one, in LT. If no drift measurements are available for the previous day, one of the quiet time empirical models of Scherliess and Fejer (1999) (S-F) or Fejer et al. (2008) (F08) is used. The main reason for

Table 1
Data Sources

Data	Source
ISR, JULIA, and ΔH data	Jicamarca Radio Observatory database http://jro.igp.gob.pe/madrigal/
IEF data	OMNIweb database http://omniweb.gsfc.nasa.gov/
Magnetic coordinates	IGRF11 http://www.ngdc.noaa.gov/AGA/vmod/igrf.html
Solar and geomagnetic indices	http://spidr.ngdc.noaa.gov/spidr/ and http://wdc.kugi.kyoto-u.ac.jp/
O/N ₂ ratio	http://guvitimed.jhuapl.edu/

using the two consecutive days is to remove the periodic condition from the old SUPIM version which may be not valid for geomagnetic storm time. For storm time conditions, the Jicamarca incoherent scatter radar $\mathbf{E} \times \mathbf{B}$ drift observations and some $\mathbf{E} \times \mathbf{B}$ drift models are used. These models are described in the following subsections.

Although it is very likely that the use of SUPIM-INPE would yield results that differ from those which could be obtained using SUPIM, the eventual changes are not determined and discussed in the present paper. The improvements of SUPIM-INPE (Santos et al., 2016; Souza et al., 2010, 2013) are surely related, as already mentioned, to the use of update models of the input parameters (neutral densities from NRLMSISE-00, EUV flux from SOLAR2000, etc.), the added calculations for a seventh ion (N⁺), and height extended calculations.

2.1. Vertical Drift Data From Jicamarca Incoherent Radar

The Jicamarca Radio Observatory (11.95°S, 78.87°W) has a 50 MHz incoherent scatter radar (ISR). This measures the vertical drift in the magnetic equator and is in operation since the 1960s. The site’s magnetic dip angle is about 1°; it slightly varies with altitude and from year to year. The vertical drifts from ISR used in this work are averages for 24 altitude steps between 218 and 577 km. The mean value of these 24 averages is the F region vertical drift. The temporal resolution is 5 min. More information about the technique and the observatory facilities can be found in Kudeki, Bhattacharyya, and Woodman (1999). All data sources used are indicated in the Table 1.

2.2. Vertical Drift From JULIA Radar

The Jicamarca Unattended Long-Term studies of the Ionosphere and Atmosphere (JULIA) system is a coherent radar which records echoes from heights between 140 and 170 km. An excellent agreement between JULIA determinations (ascribed to a nominal 150 km height) and the ISR results already mentioned has been found by Chau and Woodman (2004).

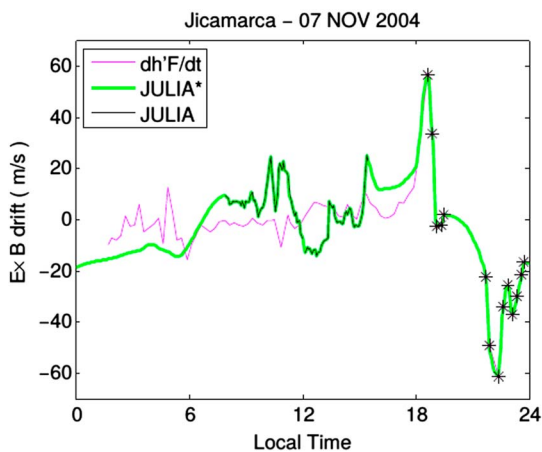


Figure 1. Composite vertical drift (JULIA*—green) for the 07 November 2004 storm at Jicamarca (11.95°S, 78.87°W) using JULIA, 07–16 LT (black); $dh'F/dt$, 18–24 LT (asterisks); and F08, 00–07 LT and 16–18 LT. Values of $dh'F/dt$ for other time intervals (magenta) are not used because heights are lower than 300 km.

The JULIA radar drift determinations are for the 07–18 LT time interval only. As SUPIM-INPE needs the full LT diurnal variation of the vertical drift, we use the time variation of the F region height ($dh'F/dt$) during the prereversal enhancement (PRE) and postsunset (18–24 LT) to partially fill in the gap. $dh'F/dt$ is calculated from the mean virtual height of reflection for 4, 5, and 6 MHz signals obtained from ionograms for the 18–24 LT time interval. Only mean heights equal or higher than 300 km are considered. A similar procedure was used by Batista et al. (2006). The F layer height variation for these heights mostly depends on the vertical drift velocities since the chemical recombination processes for this height range are less significant as shown by Bittencourt and Abdu (1981). For the 00 to 07 LT time interval, the diurnal variation is completed with the quiet condition drift models S-F or F08. This composite drift diurnal variation is denoted JULIA*. A sample JULIA* diurnal variation is given in Figure 1 for the 7 November 2004 storm: F08 model for 00–07 LT, JULIA for 07–16 LT (it should have been till 18 LT but there is no data between 16 and 18 LT, so F08 is used again), and $dh'F/dt$ for 18–24 LT. In other cases, when no data are available for the all three determinations, drift gaps have been filled in with cubic interpolations.

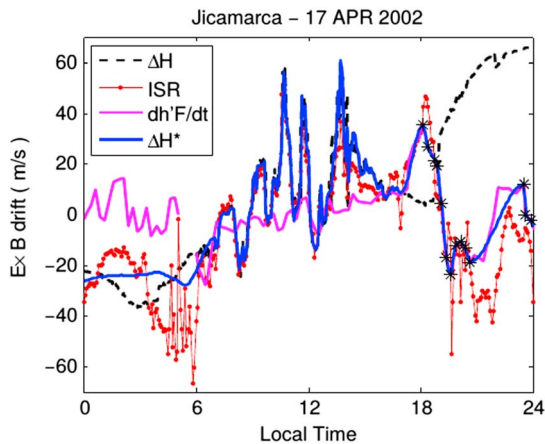


Figure 2. Composite vertical drift (ΔH^* —blue) for the 17 April 2002 storm at Jicamarca (11.95°S, 78.87°W) using ΔH , 06–18 LT (dashed black); $dh'F/dt$, 18–24 LT (asterisks); and F08 for other hours. Values of $dh'F/dt$ for other time intervals (magenta) are not used because heights are lower than 300 km. ISR drift (red).

2.3. Vertical Drift Deduced From ΔH From Magnetometers

$\mathbf{E} \times \mathbf{B}$ vertical drift is deduced from the difference between the magnetic field horizontal component measured by two magnetometers, ΔH , one located at the magnetic equator and other at a low geomagnetic latitude. Here Jicamarca (11.92°S, 78.87°W geographic; -1.55°, 352.85° geomagnetic) and Piura (5.18°S, 80.64°W geographic; 5.14°, 350.93° geomagnetic) are used. This method relies on a direct measurement of the equatorial electrojet (EEJ) current, from which the $\mathbf{E} \times \mathbf{B}$ vertical drift velocity magnitude can be estimated (Anderson et al., 2002). Some authors called this measurement as storm time EEJ index (e.g., Balan et al., 2010). Currently, one procedure to obtain the vertical drift from magnetometer observations uses a neural network technique, where the year, day of year, $F_{10.7}$ solar flux, daily A_p index, K_p index, and local time are used as inputs, as explained by Anderson et al. (2004, 2006).

The vertical drift derived from ΔH is only recommended between 07 and 17 LT as it was the case for JULIA. For other time intervals use is made of $dh'F/dt$ the S-F or F08 models so as to get a composite drift diurnal variation. This composite is denoted as ΔH^* . An example of ΔH^* is shown in Figure 2 for the 17 April 2002 storm where it is compared with the ISR vertical drift. A good agreement between the ΔH^* and ISR drifts is evident during most of the day.

2.4. Vertical Drift Derived From IEF

The drift derived from interplanetary electric field (IEF) is determined following the methodology described in Kelley and Retterer (2008) and Retterer and Kelley (2010). Efficiencies of 10% of IEF when B_z points to the south and 3% when B_z points to the north are assumed for the penetration electric field. This field is superposed to the preexisting field of quiet time conditions. The IEF is calculated according to the expression: $IEF = V_{sw}(km/s) \times B_z(nT; GST) \times 10^{-3}$ and 5 min means are computed. Moreover, there is a 15 min delay between IEF and ISR drifts. This is consistent with Kelley and Dao (2009), who suggests that there is a delay of ~10–25 min that would correspond to the slowing down of the solar wind in the bow shock and the transference times of fields to the magneto tail and to the equatorial ionosphere.

Two IEF-derived drifts are considered as applied for the 17 April 2002 storm (Figure 3). The first (IEF1) consists of using only S-F between 00 and 06 LT (it is quiet time; the storm starts at 06 LT), then S-F plus IEF at 10% efficiency when B_z points toward the south and minus IEF at 3% efficiency for positive B_z (Figure 3, left). In the second case (IEF2) F08 is used before 06 LT, then IEF at 10% efficiency from 06 to 14 (no quiet time drift added) and $dh'F/dt$ from 18 to 24 (PRE and postsunset hours). For the 14–18 interval F08 is again used just because IEF is near zero (Figure 3, right). The 15 min delay has been taken into account. The oscillations in

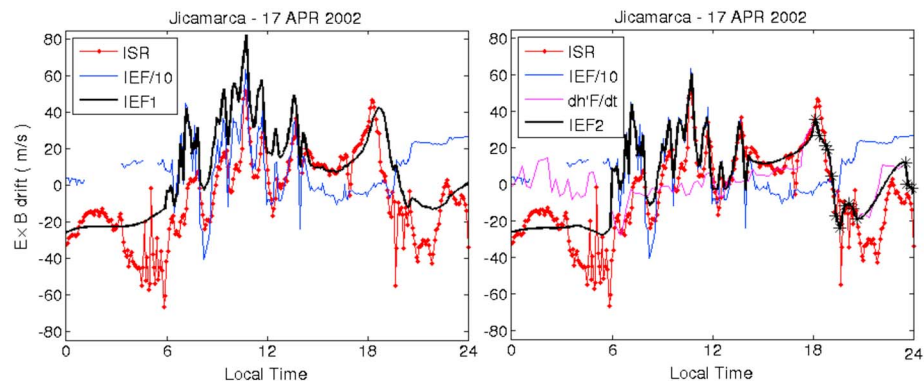


Figure 3. IEF-derived drift (black) for Jicamarca (11.95°S, 78.87°W) during 17 April 2002. IEF divided by 10 (blue) and IEF1 (left, black) and IEF2 (right, black). See text. Normal $dh'F/dt$ -derived drift (magenta) and for heights higher than 300 km (asterisks). ISR drift (red).

Table 2
List of Stations Used in the Present Work

Station	Geographical latitude	Geographical longitude	Geomagnetic latitude	Magnetic declination	DIP angle
Jicamarca (JI)	-12.0°	283.2°	0.35°	-0.01°	0.70°
São Luís (SL)	-2.5°	315.8°	-1.36°	-19.56°	-2.71°

Note. The geomagnetic coordinates are obtained for the year 2003 at 300 km height.

IEF1 and IEF2 are similar to the ones of ISR drifts, but there is a large difference in their amplitudes in the case of IEF1 drift, being approximately 30 m/s larger than the ISR one. This difference is not present in the case of IEF2. This amplitude difference seems to arise from the addition of the quiet time drift as used by Kelley and Retterer (2008). There is some similar disagreement between both IEF1 and IEF2 with ISR, but only near the first peak (06–08 LT).

A detailed investigation of the penetration IEF efficiency is not the aim of the present work; it only uses results from previous publications. However, the model has been run to include a few efficiency levels as it will be shown in the discussion.

2.5. Modeled and Observed f_oF_2 and h_mF_2

The SUPIM-INPE output parameters F layer critical frequency (f_oF_2) and peak height (h_mF_2) are compared with the corresponding Digisonde observed values. The equatorial Digisonde stations used are presented in the Table 2. The simulations for geomagnetic storms are made for two events for which ISR measurements are available (17–18 April 2002 and 7–10 November 2004). The solar flux and geomagnetic indices for those days are listed in Table 3.

While drifts are calculated in local time, the comparison between the model output and observational values are shown in universal time (UT). This is to allow the analysis of simultaneous effects of geomagnetic storms in the different stations. For the storm time simulations we consider the first storm day, when the disturbances in the vertical drift $\mathbf{E} \times \mathbf{B}$ can be mainly due to the effect of PPEF as the DD takes some hours to be effective (Abdu et al., 2006) or as soon as the disturbance wind reaches the middle latitudes (Fuller-Rowell et al., 2002).

3. Results

The SUPIM-INPE is first used for quiet geomagnetic conditions to evaluate its performance for the selected stations. The results could be considered as the SUPIM-INPE background ionosphere to be compared with the results during storm conditions for these locations.

3.1. Quiet Conditions

Figure 4 shows f_oF_2 and h_mF_2 simulations for 16 April 2002 at Jicamarca (JI; 11.95°S, 78.87°W, left) and São Luís (SL; 2.5°S, 44.2°W, right), a geomagnetically quiet day ($A_p = 7$). The first panel shows the Dst and K_p indices that characterize the time interval. The second to fourth panels correspond to the input vertical drifts and the calculated and observed values of f_oF_2 and h_mF_2 , respectively.

Table 3
Solar and Geomagnetic Indices for the Simulated Days

Date	Adjusted solar flux (W/m^2Hz)	A_p index	Minimum Dst index (nT)
16/04/2002	197.2	7	-
17/04/2002	195.0	62	-
18/04/2002	189.8	63	-127
07/11/2004	127.2	50	-
08/11/2004	131.7	140	-374
09/11/2004	138.1	119	-214
10/11/2004	102.6	161	-263

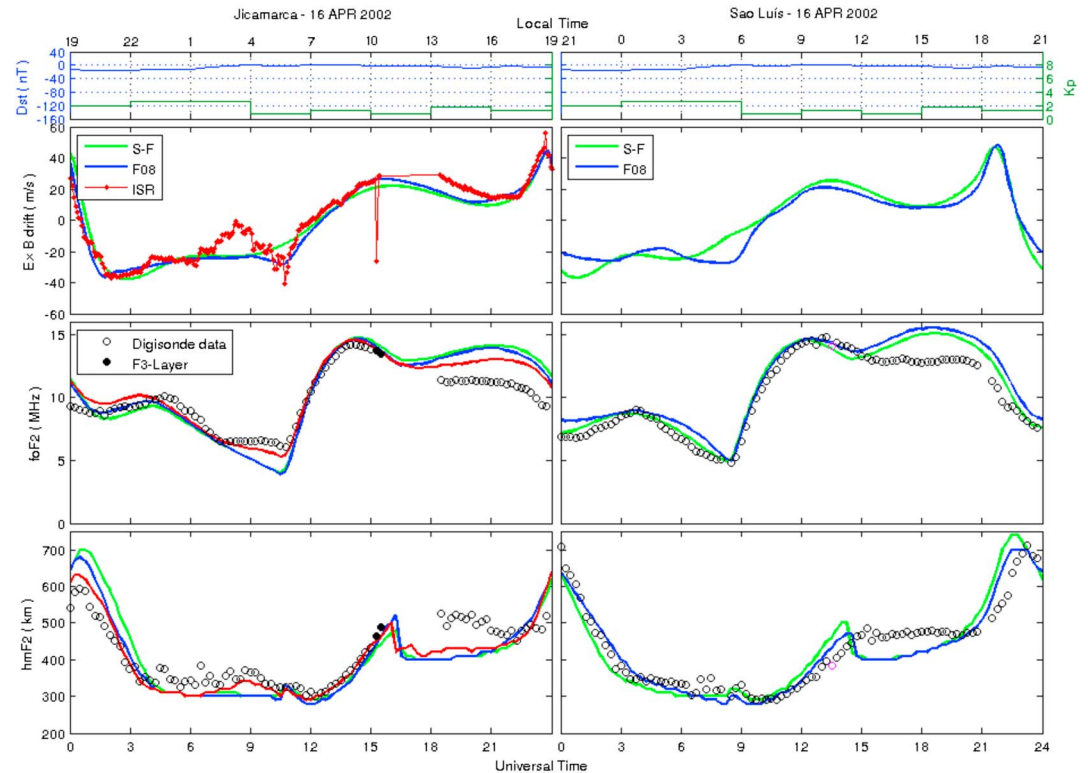


Figure 4. Simulated (lines) and observed f_oF_2 and h_mF_2 (circles) over Jicamarca (11.95°S, 78.87°W, left) and São Luís (2.5°S, 44.2°W, right) for 16 April 2002. (first panel) Dst and Kp . (second panel) Input vertical drifts: S-F (blue), F08 (green), and ISR (red oblongs, Jicamarca only). (third panel) f_oF_2 and (fourth panel) h_mF_2 . F_3 layer (filled circles).

The S-F and F08 drifts are very similar to each other and also generally similar to the ISR drift for JI. The main differences are between S-F and F08 for some hours after midnight (10–12 UT at JI and 00–02 and 07–09 for SL). There are also differences between S-F and ISR at JI (07–09 UT). Drifts for other quiet days give similar results, though there is some variability on the timing of largest differences.

Simulated f_oF_2 and h_mF_2 for all three drifts used are fairly similar. Larger differences are found between f_oF_2 derived from ISR and S-F or F08 at JI just before sunrise (08 to 11 UT) and in the afternoon (18–22 UT). It is noteworthy that drift differences already indicated do not translate into simulated f_oF_2 differences. Neither is the ISR drift point out of the trend 15 UT. SL simulated f_oF_2 using S-F and F08 are closer than for JI all day long. Simulated h_mF_2 using all three drifts for JI are very close indeed. The larger differences occur in the evening (00–03 UT), h_mF_2 being largest for S-F than for F08 and ISR. The same is approximately true for S-F and F08 at SL.

There is a generally good agreement between the simulated f_oF_2 and h_mF_2 and those observed at JI and SL, particularly between the simulated characteristics using ISR drift for JI. The after midnight and early morning (00–16 UT) simulations are better than those for other hours. After 16 UT in SL and 18 UT in JI (there is no observations between 16 and 18 UT) the differences reach up to 3 MHz in f_oF_2 and 100 km in h_mF_2 . This disagreement was also reported by Souza et al. (2013). They explained that during this time interval the F_3 layer formation process, a combined $\mathbf{E} \times \mathbf{B}$ drift and thermospheric neutral winds effect close to the magnetic equator (Balan & Bailey, 1995), is generally very active. The process is not well reproduced by SUPIM-INPE. It is just after 15:00 UT that a F_3 layer is observed over JI. As thermospheric winds are a key factor on the F_3 layer formation, it is possible that the HWM93 used in the present simulation is not representing the wind well. The F_3 layer had already been observed in Jicamarca (11.95°S, 78.87°W), Trivandrum (12°N, 77°E), and Fortaleza (3°S, 38°W) during quiet conditions, reaching heights between 450 km and 600 km when it is strongest, according to simulation results from Balan et al. (1997). The F_3 layer formation could also produce some disagreements between simulations and observations in the

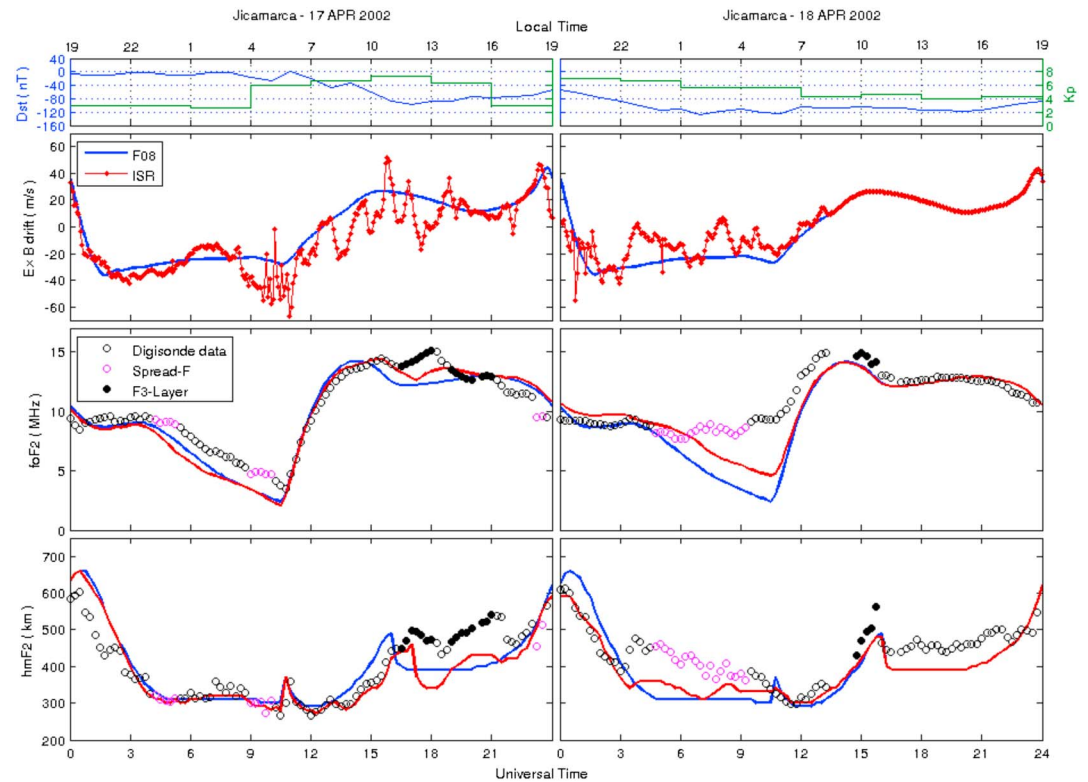


Figure 5. Simulated (lines) and observed f_oF_2 and h_mF_2 (circles) over Jicamarca (11.95°S, 78.87°W) for (left) 17 April 2002 and (right) 18 April 2002. (first panel) Dst and Kp . (second panel) Input vertical drifts: F08 (blue) and ISR (red oblongs) up to 13:25 UT, then idem to F08. (third panel) f_oF_2 and (fourth panel) h_mF_2 . F_3 layer (filled). Spread F (magenta).

afternoon during storms, and possibly, the disturbed $\mathbf{E} \times \mathbf{B}$ drift and neutral winds could generate F_3 layer in other hours as well. A comprehensive theoretical study of the F region during strong storm for equatorial and middle latitudes is reported by Lin, Richmond, Liu, et al. (2009). They find the split of the F region into F_2 and F_3 layer during the day over a wide range of latitudes, with F_3 layer heights in the 1500–2000 km range.

It is recalled that comparisons between ISR, ΔH^* , and dh'/dt drifts were made for 17 April 2002, a disturbed day. Comparisons have also been made for the previous day, a quiet one. The results are similar, namely, that for 07–17 LT ISR and ΔH^* are almost the same, and so are ISR and dh'/dt for the 18–23 LT time interval, albeit some minor exceptions. This confirms that use can be made of these drifts to complete the diurnal variations during quiet times. The SUPIM-INPE f_oF_2 and h_mF_2 simulations using these drifts do not lead to significant differences (not shown).

In general, the SUPIM-INPE responds well during the geomagnetic quiet conditions. The ΔH drift together dh'/dt observations and quiet time models (ΔH^*) are a good substitute for the quiet conditions.

3.2. The 17–18 April 2002 Storm

The geomagnetic storm of 17–18 April 2002 is produced by the arrival of a coronal mass ejection (CME) to the Earth. The ACE satellite registers this arrival on 17 April at 11:00 UT with the change of the z component of magnetic field to southward (Goncharenko et al., 2005). This geomagnetic storm is classified as moderate.

Figure 5 shows simulated and observed f_oF_2 and h_mF_2 for Jicamarca during the storm, using F08 and ISR drifts. Since ISR drifts are available only till 18 April at 13:25 UT, F08 values are used for the rest of that day.

Before the beginning of the storm, the simulations computed using the two drifts are similar as expected for quiet times. After that, between 11 and 20 UT, the ISR drift oscillations do not translate into the f_oF_2

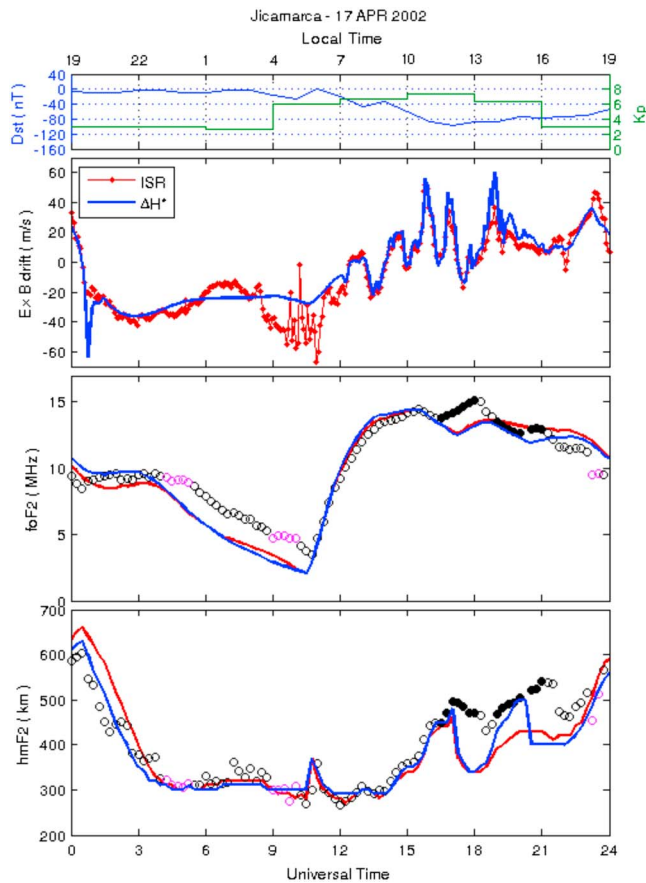


Figure 6. Simulated (lines) and observed f_oF_2 and h_mF_2 (circles) over Jicamarca (11.95°S, 78.87°W) for 17 April 2002. (first panel) Dst and Kp . (second panel) Input vertical drifts: ΔH^* (blue) and ISR (red oblongs). (third panel) f_oF_2 and (fourth panel) h_mF_2 . F_3 layer (filled). Spread F (magenta).

simulations. They rather seem to closely follow those simulated using quiet drift model. By contrast, such drift oscillations do affect the simulated h_mF_2 .

When f_oF_2 and h_mF_2 simulations are compared with observations, a good agreement between the two is found for several hours after of beginning of the storm. However, some amplitude differences can be seen in the afternoon (17–22 UT). As already mentioned, these could be explained by F_3 layer formation processes. During the night, between 22 and 07 UT for f_oF_2 and between 22 and 03 UT for h_mF_2 , the simulations again reproduce the observations well.

During 18 April the relation between drifts and simulated f_oF_2 and h_mF_2 is similar to that for 17 April as indicated above. However, the observed f_oF_2 does not show the characteristic minimum before dawn, which is well reproduced by the simulated f_oF_2 using both input drifts. Rather, it oscillates at about 9 MHz with periods that resemble the ISR drift variations. In the case of h_mF_2 , observations between 03 and 10 UT show values higher than those expected from simulations and for observed previous normal conditions. Also, spread F is prevalent for the same time interval. This spread F may have been generated by a DD electric field, which starts some hours after the onset of the storm, and has opposite phase to the quiet time dynamo electric field (Abdu et al., 2006; Fuller-Rowell et al., 2002). The DD in this case does seem to occur between 03 and 06 UT and between 07 and 08 UT, when the vertical drifts are much higher than during quiet time. Although the ISR measured drifts were used in the simulation, SUPIM-INPE does not reproduce well this observed behavior probably due to the combined action of an equatorward disturbed wind, which was not taken into account in the present simulation.

An alternative drift model to be evaluated is the ΔH^* , which was constructed as described previously (section 2.3). The comparison between the f_oF_2 and h_mF_2 simulations using ΔH^* drift and ISR drift is shown in Figure 6. As expected, the simulations using both drifts are similar and the difference between the drifts at night (06–11 UT) does not generate

significant differences in the corresponding f_oF_2 and h_mF_2 simulations. Furthermore, the observed f_oF_2 and h_mF_2 differ from the simulations in a similar way than shown in Figure 5. The simulation is not carried out for São Luis because ΔH^* drift is not available for that location.

Another drift model to be used in the simulation is the one deduced from IEF data. The f_oF_2 and h_mF_2 simulations for Jicamarca with these drifts are shown in Figure 7. The simulations using IEF1 and IEF2 are presented together with those using ISR drifts. Note that although ΔH^* and IEF2 drifts use dh'/dt observations during hours of PRE and postsunset, only for the ΔH^* drift case is used for the previous day. This is the reason for the differences around 01 UT between ΔH^* drift (Figure 6) and IEF2 drift (Figure 7). The simulations show that during nighttime (00–11 UT) there are no significant differences between results derived using IEF1, IEF2, or ISR drifts. This is because all the three vertical drifts are for quiet conditions. At the beginning of the storm (11–14 UT), all three f_oF_2 simulations are also similar and reproduce the observations well. But later (14–21 UT), the simulation using the IEF1 drift shows f_oF_2 up to 3 MHz lower than the observations. That is even lower than the simulations using ISR. This disagreement becomes less pronounced when the IEF2 drift is used.

In the case of the h_mF_2 simulations, during the storm main phase (11–16 UT), the use of IEF1 and IEF2 drifts leads to higher simulated h_mF_2 relative to the simulations using ISR and also to observed values. The very high peak at 16 UT is generated by the high values of IEF1 drift at this hour. The differences between h_mF_2 simulations and observations are smaller when the IEF2 drift is used.

The drift inferred from the IEF seems to be a good substitute (perhaps with some modifications) when the ISR drift is not available, but it is not better than the ΔH^* drift.

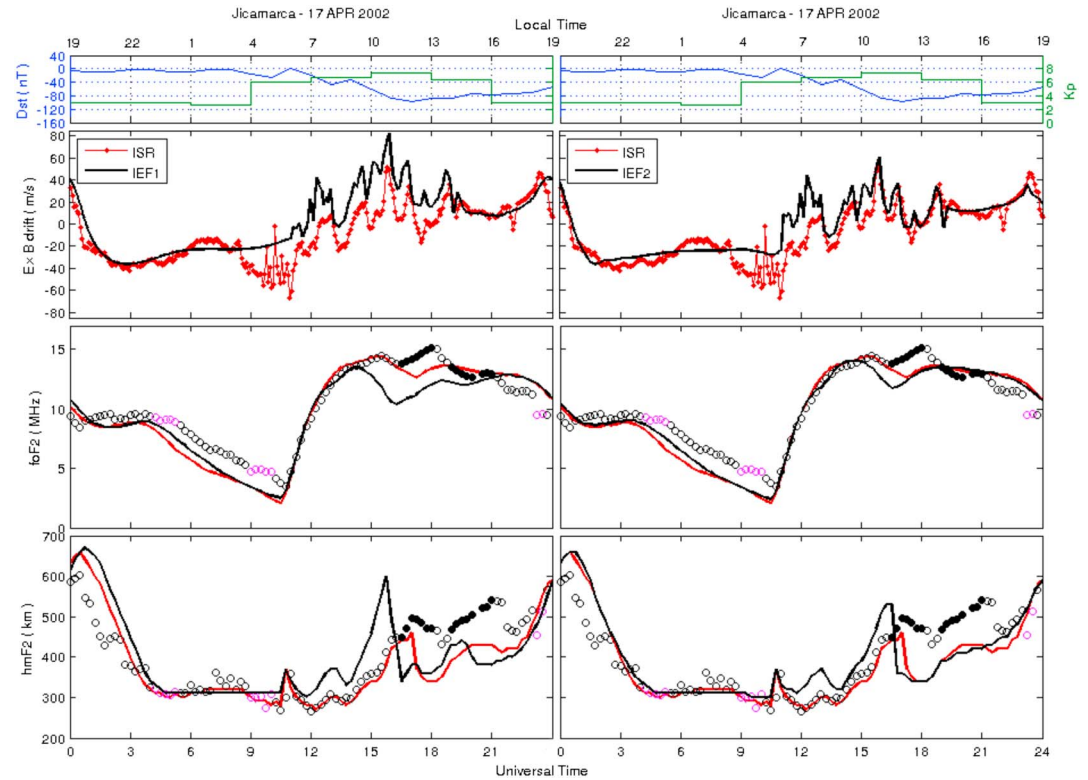


Figure 7. Simulated (lines) and observed f_oF_2 and h_mF_2 (circles) over Jicamarca (11.95°S, 78.87°W) for 17 April 2002. (first panel) Dst and Kp . (second panel) Input vertical drifts: IEF1 (black, left), IEF2 (black, right), and ISR (red oblongs). (third panel) f_oF_2 and (fourth panel) h_mF_2 . F_3 layer (filled). Spread F (magenta).

Based on the assumption that the prompt penetration electric field, in the initial phase of the magnetic storm, is the responsible for producing the disturbances in the zonal electric field at the equator (neglecting any significant longitudinal variation), we developed a methodology to obtain drift for the São Luís equatorial station from Jicamarca ISR values. This consists on removing the quiet time variation (using the F08 model) from the Jicamarca ISR measured during the storm, and adding the São Luís quiet variation to the residue. The vertical drift for SL calculated using this approach is presented in the second panel of Figure 8 and denoted ISR^* . IEF1 and IEF2 drifts calculated for SL are also shown. So are the corresponding f_oF_2 and h_mF_2 simulations for each drift model.

As we can see, the simulations using the ISR^* drift for SL reproduced very well the observations during the storm time, except during the PRE (21–24 UT), where the simulated h_mF_2 is higher than the observations for up to 150 km. For the IEF1 drift, the f_oF_2 simulation is lower (~3 MHz) than observations during all the storm time and the h_mF_2 simulation presented three peaks not seen on the observational data nor on the simulations using ISR^* . On the other hand, the simulations using IEF2 drifts show a better agreement with the observed f_oF_2 and there is only one disagreement peak for h_mF_2 . During the PRE hours IEF2 drift simulations reproduce the observations well. In fact, in this time interval, IEF2 drift is based on dh'/dt from ionograms at SL, as described in section 2.4.

In conclusion, the methodology to determine a disturbance vertical drift for 17 April at SL from Jicamarca ISR leads to good results, except for the PRE hours where, as demonstrate by the IEF2 model, it is better to use the dh'/dt . However, the IEF2 drift model is found to be efficient too and could be a good substitute model for those times and locations for which ISR measurements are not available.

3.3. The 7–10 November 2004 Storm

The geomagnetic storm of 7–10 November 2004 is produced by various solar flares accompanying CMEs that arrived at Earth. The beginning of this storm is registered by three sudden commencement pulses on 7

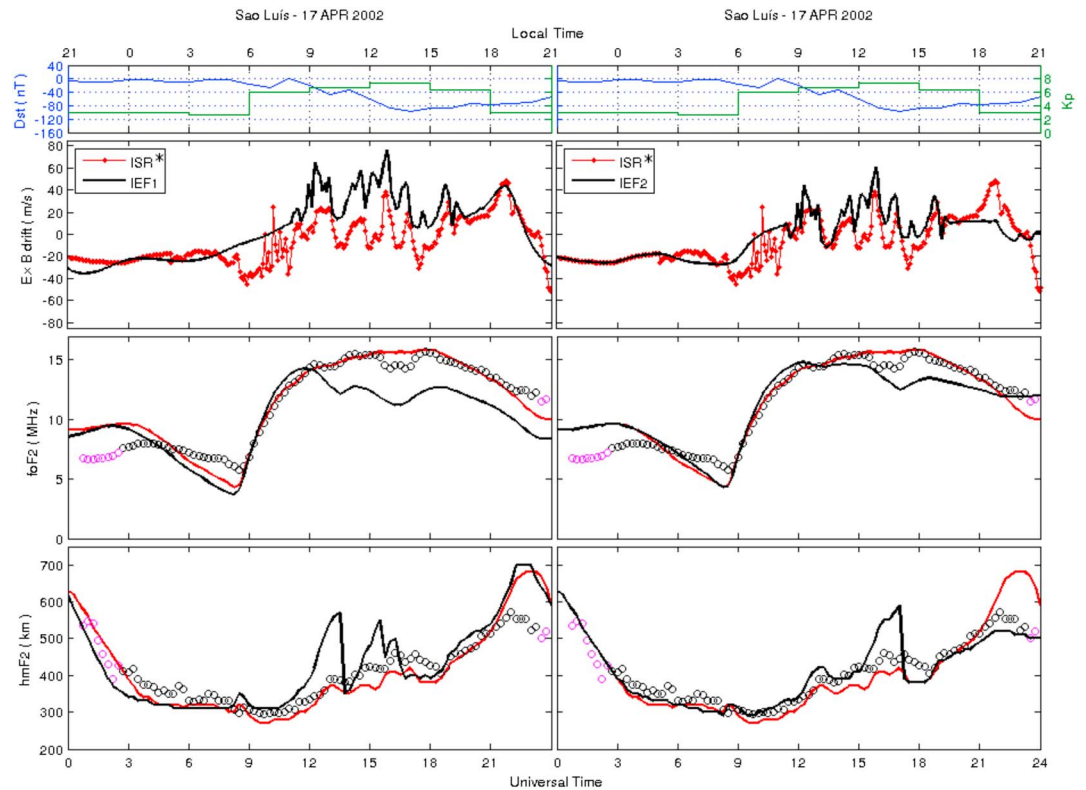


Figure 8. Simulated (lines) and observed f_oF_2 and h_mF_2 (circles) over São Luís (2.5°S, 44.2°W) for 17 April 2002. (first panel) Dst and Kp . (second panel) Input vertical drifts: IEF1 (black, left), IEF2 (black, right), and ISR* (red oblongs). (third panel) f_oF_2 and (fourth panel) h_mF_2 . F_3 layer (filled). Spread F (magenta).

November at 02:58, 11:13, and 18:31 UT and other register on 9 November at 18:52 UT (Panasencko & Chernogor, 2007). This geomagnetic storm was classified as superintense (Echer, Gonzalez, & Tsurutani, 2008).

Figure 9 shows simulated and observed f_oF_2 and h_mF_2 for Jicamarca during 9 and 10 November using S-F, F08, and ISR drifts. Since ISR drifts are available from 12 UT of 9 November, F08 is used before then.

The disagreement between simulations and observations observed after midnight (up to 12 UT) could be attributed to the fact that quiet time drifts have been used to simulate an already disturbed environment. The storm had already begun 2 days before. During the 9 November daylight hours (after 12 UT), the f_oF_2 simulations underestimate the observations for up to 4 MHz. In the case of h_mF_2 , simulations are in good agreement with observations. This suggests that the large f_oF_2 discrepancies could be attributed to disturbance neutral winds. It is noteworthy that SUPIM-INPE reproduces the h_mF_2 observed peak around 20–21 UT and the large f_oF_2 trough associated with the occurrence of a F_3 layer.

The PRE is strongly inhibited in 9 November, as clearly shown by the ISR observations. However, this may not always be the case as the DD may tend to enhance it (i.e., Maruyama et al., 2005). Here the simulated f_oF_2 are smaller than the observations, much as they were before the PRE. The h_mF_2 simulations, however, are closer to the observations.

Unfortunately, there is a several hour gap in the f_oF_2 and h_mF_2 observations during nighttime (10 November 04–13 UT). Before the gap, observed f_oF_2 somewhat follows the decreasing trend shown by the simulations, particularly those done using S-F and F08. h_mF_2 , however, agrees well with ISR-derived simulations. It is possible that the great variations of the ISR drift in this time interval could be due to DD effects, although as B_z and AE index also vary in these hours, it may be also the effect of the PPEF or the effect of both.

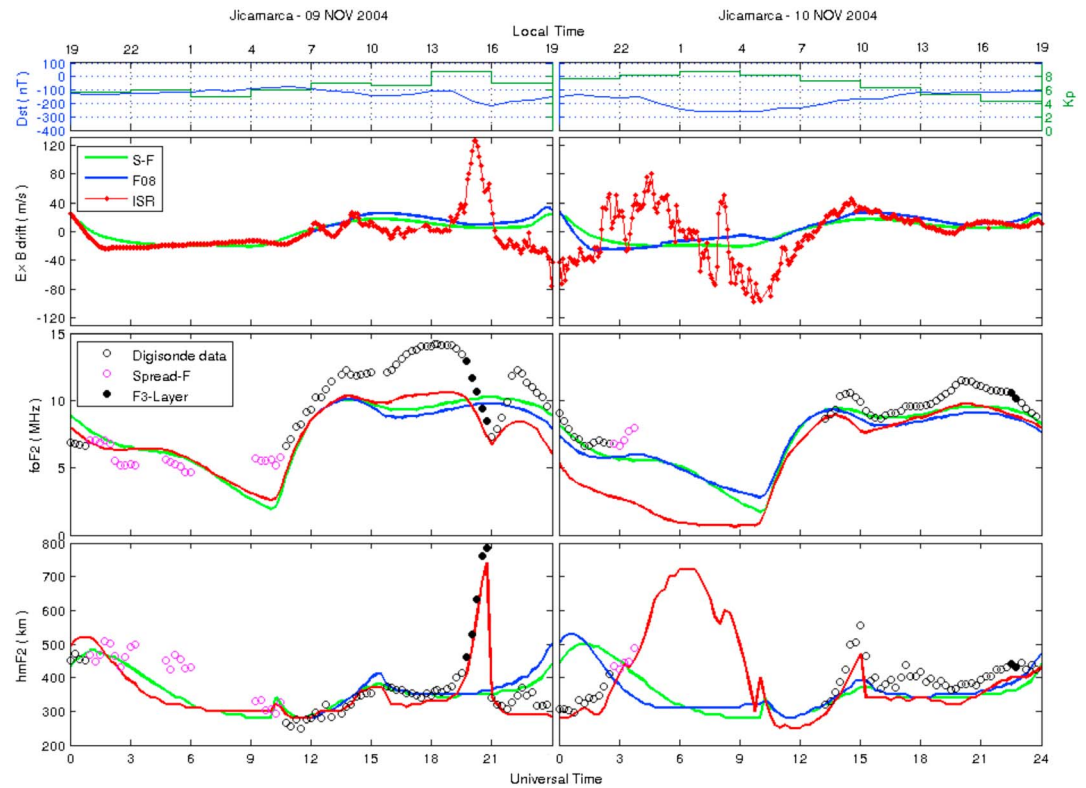


Figure 9. Simulated (lines) and observed f_oF_2 and h_mF_2 (circles) over Jicamarca (11.95°S, 78.87°W) for (left) 09 November 2004 and (right) 10 November 2004. (first panel) Dst and Kp . (second panel) Input vertical drifts: S-F (green), F08 (blue), and ISR (red oblongs). (third panel) f_oF_2 and (fourth panel) h_mF_2 . F_3 layer (filled). Spread F (magenta).

During 10 November daylight hours (after the gap), f_oF_2 and h_mF_2 simulations are closer to observations. This is true for both quiet time-derived drifts and observed ISR drift.

Figure 10 shows again simulated and observed f_oF_2 and h_mF_2 for Jicamarca during 9 November. This time, however, simulations are done using the vertical drift ΔH^* , as determined for the 17–18 April 2002 storm. A slightly better agreement is observed at nighttime, more noticeable for h_mF_2 . This is because dh'/dt is used to represent the composite ΔH^* drift. During the rest of the day ΔH^* drift simulations are very similar to those using the ISR data. Note the agreement for the f_oF_2 trough and h_mF_2 peak.

Simulations of f_oF_2 and h_mF_2 using the vertical drifts IEF1 and IEF2 are now considered as depicted in Figure 11. IEF2 simulations are closer to ISR simulations than IEF1 are, in the same way that IEF2 and IEF1 drifts are to the observed ISR drift. This fact translates into the f_oF_2 and h_mF_2 observations; for example, IEF2-derived simulations are generally closer to observations than are those using IEF1, the exception probably being at the 20 UT peak. However, the ISR-derived simulations are still better than the IEF2 ones, albeit they are not very good themselves.

As previously described, it is possible to obtain a disturbance vertical drift for SL from ISR observations, the so-called ISR*. The results for 9 November (given in the supporting information) show a disagreement between simulation and observations in the early hours due to absence of ISR observations. Although during daylight f_oF_2 simulations underestimate the observations by up to 4 MHz, h_mF_2 simulations agree with observations, the peak observed around 20–21 UT being also reproduced albeit but higher values. For the simulations with IEF2 drift the agreement with observation is worse. This may be due to the absence of dh'/dt values for heights higher than 300 km.

Finally, JULIA* drift could be used for Jicamarca, although only for 7 November. The computations are made as described in section 2.2 (see Figure 1). Figure 12 shows that simulated f_oF_2 are almost always underestimated. However, there is a remarkable agreement between h_mF_2 simulations and available observations.

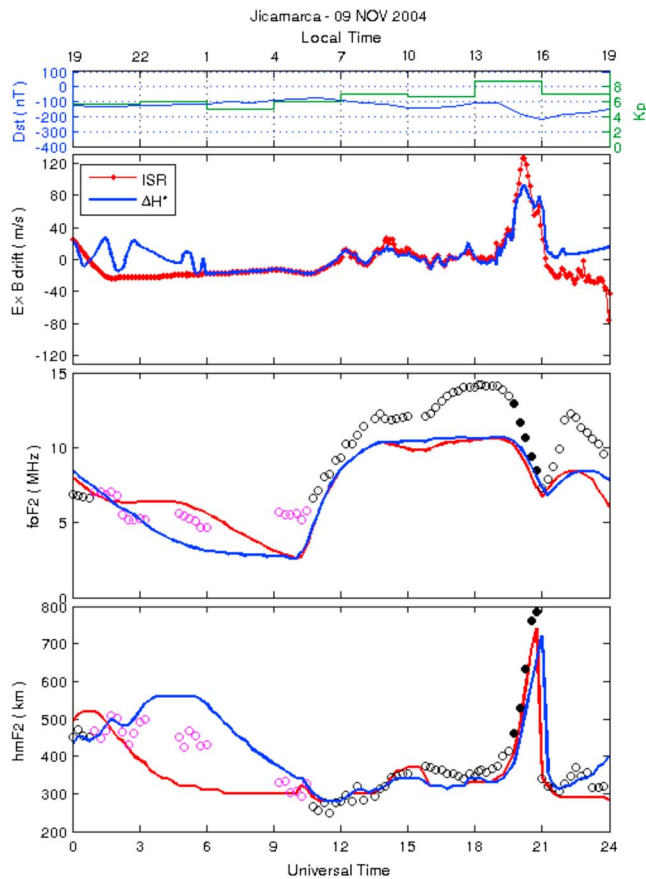


Figure 10. Simulated (lines) and observed f_oF_2 and h_mF_2 (circles) over Jicamarca (11.95°S, 78.87°W) for 09 November 2004. (first panel) Dst and K_p . (second panel) Input vertical drifts: ΔH^* (blue) and ISR (red oblongs). (third panel) f_oF_2 and (fourth panel) h_mF_2 . F_3 layer (filled). Spread F (magenta).

This good agreement suggests that the f_oF_2 disagreements could be attributed to disturbed winds, which are not being considered in the present simulation.

In summary, based on the comparisons presented, it is possible to conclude that the best model disturbance drift for the 7–10 November 2004 storm is ΔH^* , followed by the IEF2 and finally the IEF1 drift. The same result already reached at for the 17–18 April 2002 storm.

4. Discussion

The PPEF during the geomagnetic storm of 17 April 2002 was captured by numerous ground and satellite instruments. The equatorial electric field was measured by the ISR at Jicamarca and at Sondrestrom (Kelley et al., 2003); it was registered by the ΔH variations from magnetometers and is also present in the IEF signatures of the ACE satellite measurements. The comparisons of these drifts during the 17 April 2002 are shown in Kelley et al. (2003) and Anderson et al. (2004). A maximum correlation coefficient of 0.773, with a delay of 10 min, is found between the IEF and ISR in Kelley et al. (2003), with an efficiency rate of 7%. Note that here we have used a 10% efficiency rate. Denardini et al. (2011) calculated the ΔH drifts deduced for the Brazilian sector during the 17 April 2002 and 31 March 2001 storms and compared them with the IEF values. They found an efficiency of 11%.

A strong coupling between the magnetosphere and the ionosphere is observed in the events of 7–12 November through the PPEF. The behavior of the ionosphere during this event has been modeled by some authors. For example, Balan et al. (2009) modeled the effects of the PPEF event during the geomagnetic storm of the 9 November 2004 using SUPIM. They used the $\mathbf{E} \times \mathbf{B}$ drift velocity measured in Jicamarca (ISR) with and without an equatorial wind as input. They concluded that a superplasma fountain is produced when the PPEF acts in the presence of an equatorward wind. If we compare the Balan et al. (2009) simulation results at the geomagnetic

equator (0°, Jicamarca), the simulated electron density minimum was produced at 17 LT, while, as already mentioned, in this work it was at 16 LT (Figure 9), which agrees with the f_oF_2 observations (circles). This can be due to some updates/improvements made in SUPIM-INPE or to the use of quiet winds instead of the disturbance wind proposed by Balan et al. (2009).

Simulations for 8 November 2004, with SUPIM, were made by Balan et al. (2013) for the Japan–Australia sector (135°E). They concluded that either zero or westward electric fields can contribute the positive storms, although they do not act independently of the neutral wind. Equatorward neutral winds are present simultaneously, and its downwelling effect increases O/N_2 ratio round the equator contributing to the positive storms by increasing daytime production of ionization. The SUPIM-INPE uses as input the NRLMSISE-00, and this model does incorporate an O/N_2 ratio increase for geomagnetic activity increases. The TIMED/GUVI observations also show O/N_2 ratio increases during storms. However, it is fair to say that observed increases are larger than the model increases for the specific geomagnetic storms studied in the present paper. These changes in the O/N_2 ratio could affect the equatorial ionosphere some hours after the beginning of the storm, in the recovery phase.

The electric field disturbances produced by the DD, which occur some hours after the beginning of the storm, were not considered in the IEF-derived drifts. It should be noted, however, that they are obviously included in the ISR, JULIA, dh'/dt , and ΔH observations. In the events analyzed here it seems that the DD is present 4 h after the storm onset, around the 23 UT of 7 November 2004 (Figure 12), which was inferred from the lower than normal F layer heights both at São Luis and Fortaleza (Abdu et al., 2006). For this reason, in this work only the first day of the storm is used (17 April, 7 and 9 November).

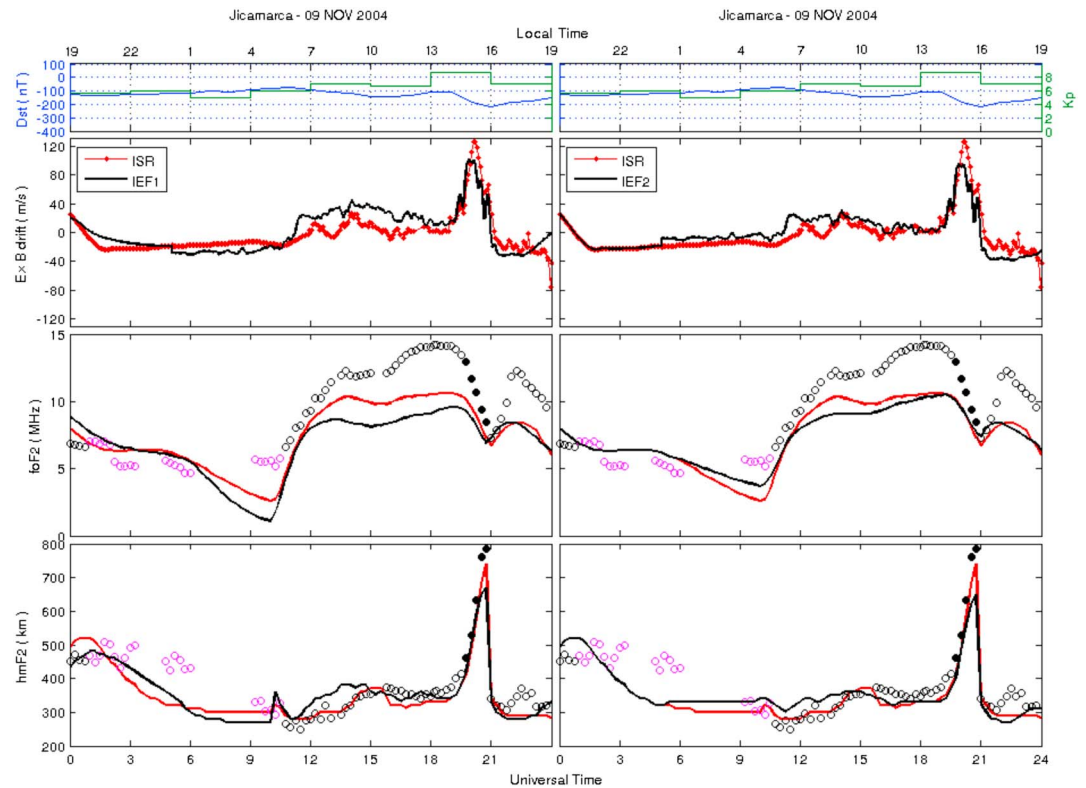


Figure 11. Simulated (lines) and observed f_oF_2 and h_mF_2 (circles) over Jicamarca (11.95°S, 78.87°W) for 09 November 2004. (first panel) Dst and Kp . (second panel) Input vertical drifts: IEF1 (black, left), IEF2 (black, right), and ISR (red oblongs). (third panel) f_oF_2 and (fourth panel) h_mF_2 , F_3 layer (filled). Spread F (magenta).

Simulations for the St. Patrick superstorm (17–18 March 2015) using SAMI2 (Sami2 is Another Model of the Ionosphere) over the Indian region are reported by Joshi et al. (2016). They use a composite vertical drift model: for 18–21 IST (UT + 5:30) a vertical drift derived from HF Doppler observations (Tirunelveli; 8.5°N, 78.2°E; 0.5° geomagnetic latitude) of F layer height at 7 MHz in association with standard ionogram $h'F$ and f_oF_2 determinations is used; for all other times the quiet time S-F model applies. They show modeling results for altitude versus latitude displays for specific hours rather than comparison with hourly f_oF_2 and h_mF_2 observations. A clear dynamical behavior of EIA during 12–20 IST for the storm phases is seen: enhancements in the main phase (concentration and height) and almost complete suppression during recovery phase after 17 IST. Model total electron content (TEC) (integration from 100 to 1500 km) and observed GPS TEC are also compared. Unfortunately, direct comparison to our results is not readily possible.

It can be noted that some small differences between the IEF1 drifts of this work (left plot of Figure 3 and left and top plots of Figure 11, black curves) and the calculated drifts in Retterer and Kelley (2010) (Figures 3 and 8 of Retterer & Kelley (2010), green curves) could be observed. These small differences are due the IEF data source used. They worked directly with ACE satellite data, while we have worked with the averaged data obtained from the OMNIweb database.

The Kelley and Retterer model (IEF1) considers the disturbance drift as a perturbation produced by the PPEF over the quiet ionospheric dynamo in the equatorial station; however, it can be seen that this drift is overestimated with respect to the ISR data around 20–30 m/s (except in the peak on 9 November at 20 UT). These overestimated values could be due to the presence of a DD, which would help to reduce the amplitude of the drift values. Under this assumption, in Retterer and Kelley (2010) a disturbance drift model developed by Fejer and Scherliess (1997) is used for the determination of IEF1 on 17 April and it includes the effects of the DD. The disturbance model of Fejer and Scherliess (1997) is an empirical model based in the ISR data, correlated and parameterized by AE index. However, the amplitude of the new IEF1

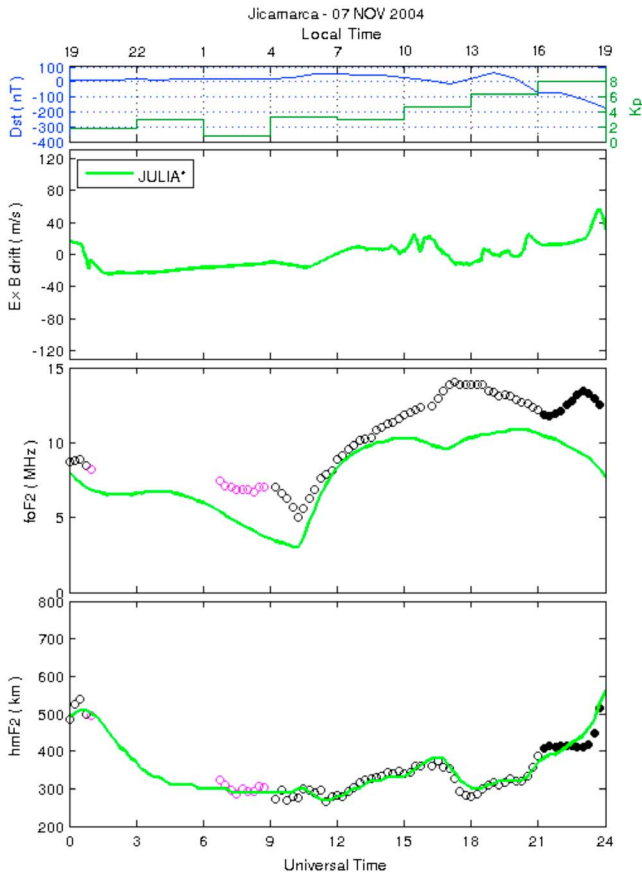


Figure 12. Simulated (lines) and observed f_oF_2 and h_mF_2 (circles) over Jicamarca (11.95°S, 78.87°W) for 07 November 2004. (first panel) Dst and Kp . (second panel) Input vertical drift: JULIA* (green). (third panel) f_oF_2 and (fourth panel) h_mF_2 . F_3 layer (filled). Spread F (magenta).

drift is slightly less than IEF1 of left plot of Figure 3 (or left plot of Figure 7) and remains overestimated with respect to the ISR data.

The IEF2 drift, which is a modification of the IEF1 drift model, does not include the effect of the ionospheric dynamo having a better response than IEF1 when simulated results are compared to observations. It is important to remember that, in the hours of the PRE and after sunset, $dh'F/dt$ values are used to compose the IEF2 model. A possible source of disagreement between the drift calculated using IEF data could be the efficiency of 10 and 3% that was used here, following Kelley and Retterer (2008) model.

As mentioned before, there are some works that determine other efficiency values for IEF. For example, Huang et al. (2010) analyzed the plasma drift and ionospheric electric field data measured near the dusk meridian at the magnetic equator by the Defense Meteorological Satellite Program F13 satellite, during four storms having $Dst < -200$ nT (6 April 2000, 17 September 2000, 30 March 2001, 29 October 2003) and compared with the IEF data. They found an efficiency of 5% of IEF for eastward and 10% of IEF for upward components of ionospheric electric field. Wei et al. (2008) deduced an average efficiency of 13.6%, albeit for the reconnection electric field in ISR during 125 h of penetration for the 11–16 November 2003 magnetic storm. They also deduced a high local time dependence for this event. The local time dependence was reported before by Fejer et al. (2007) for the November 2004 magnetic storm. Further, Kelley et al. (2003) found an efficiency of 6.6% of IEF, Burke et al. (2007) found an efficiency of 11.9%, and Huang et al. (2007) found an efficiency of 9.6% for rapid southward turning of the IMF, among others. Furthermore, according to Fejer et al. (2007) the relationship between equatorial prompt penetration electric fields and solar wind electric field effects and solar wind and reconnection electric field and polar cap potential drops is far more complex than implied by simple proportionality factors.

We have now determined the efficiencies for the best correlation between IEF1/IEF2 and ISR. For a fixed efficiency corresponding to a northward B_z the other efficiency (for southward B_z) was changed till the best fit was obtained (largest correlation coefficient). Then, for that efficiency the efficiency for northward B_z was modified so as to get a still better correlation coefficient. It is found that although the new efficiencies are different from the 10% and 3% used before, the corresponding correlation coefficients are not significantly different. The corresponding changes for f_oF_2 and h_mF_2 determined using SUPIM-INPE are very slightly better. Table 4 compares the efficiencies and correlation coefficients found for IEF1 and IEF2 models, and a figure equivalent to Figure 7 is given as supporting information.

On the other hand, with respect to the methodology for obtaining the drift for São Luis (ISR* drift), this is consistent with the formulation of the Kelley and Retterer (2008) model (IEF1), because the anomaly produced by the PPEF is removed from ISR data and added to the quiet drift of São Luis.

Table 4
Efficiency Test

Dates, IEF efficiencies (%), and correlation coefficients (R)	17 April 2002			09 November 2004		
	Southward B_z	Northward B_z	R	Southward B_z	Northward B_z	R
IEF1 model (Kelley & Retterer, 2008)	10	3	0.77	10	3	0.70
IEF2 model	10	3	0.81	10	3	0.75
IEF1 model best fit	5	3	0.79	13	4	0.73
IEF2 model best fit	9	2	0.82	13	3	0.76

5. Conclusions

The equatorial ionosphere response to different disturbed electric field models is analyzed using SUPIM-INPE. The aim is to find the better electric fields that provide good temporal and spatial coverage, and could be used as input parameters for ionospheric models, in absence of incoherent scatter radar measurements.

The f_oF_2 and h_mF_2 simulations showed that the composite ΔH^* and JULIA* drifts are the better alternatives to ISR drift. The best agreements between simulations and observations are obtained during daytime (6–18 LT), PRE hours, and after the sunset (18–24 LT) because $dh'F/dt$ is used. When such measurements are not available, the IEF drift model can be used with advantage for the good temporal availability of the data. The methodology to deduce vertical drift from IEF may vary in each case with efficiencies between 3% and 14% of IEF and a possible local time dependency. Our simulation results showed that, for some cases, the addition of the quiet time electric field as background is not necessary. Otherwise, if the PPEF is the source of disturbance electric field, it is possible to extract the anomaly of diurnal variation measured in some equatorial station and use the disturbed part to deduce the electric field at some other equatorial station without measurements, as it was done for São Luis.

Acknowledgments

Manuel Bravo would like to thank CNPq and CAPES Brazilian agencies for the financial support for doctoral studies in INPE. I.S.B. acknowledges CNPq through grants 474351/2013-0, 4000373/2014-9, 303461/2014-4, and 302920/2014-5 for the support. J.R.S. was supported by a CNPq grant 305885/2015-4. We thank Percy Condor and Jicamarca Radio Observatory for the multiple data used. We also thank Maria Goreti from INPE for the help in Digisonde data reduction. Manuel Bravo also thanks the AFOSR grant project FA9559-14-1-0139 in the USACH for the support and time used in write this paper. Finally, we acknowledge all data sources listed in Table 1. Comments received from two referees which led to several text changes are most welcomed.

References

- Abdu, M. A. (2005). Equatorial ionosphere–thermosphere system: Electrodynamics and irregularities. *Advances in Space Research*, *35*, 771–787. <https://doi.org/10.1016/j.asr.2005.03.150>
- Abdu, M. A., de Souza, J. R., Sobral, J. H. A., & Batista, I. S. (2006). Magnetic storm associated disturbance dynamo effects in the low and equatorial latitude ionosphere. In B. Tsurutani, R. McPherron, G. Lu, J. H. A. Sobral & N. Gopalswamy (Eds.), *Recurrent magnetic storms: Corotating solar wind streams*. Washington, DC: American Geophysical Union. <https://doi.org/10.1029/167GM22>
- Anderson, D., Anghel, A., Chau, J., & Veliz, O. (2004). Daytime vertical $E \times B$ drift velocities inferred from ground-based magnetometer observations at low latitudes. *Space Weather*, *2*, S11001. <https://doi.org/10.1029/2004SW000095>
- Anderson, D., Anghel, A., Chau, J. L., & Yumoto, K. (2006). Global, low-latitude, vertical $E \times B$ drift velocities inferred from daytime magnetometer observations. *Space Weather*, *4*, S08003. <https://doi.org/10.1029/2005SW000193>
- Anderson, D., Anghel, A., Yumoto, K., Ishitsuka, M., & Kudeki, E. (2002). Estimating daytime vertical $E \times B$ drift velocities in the equatorial F -region using ground-based magnetometer observations. *Geophysical Research Letters*, *29*(12), 37-1-4. <https://doi.org/10.1029/2001GL014562>
- Bailey, G. J., & Balan, N. A. (1996). Low-latitude ionosphere-plasmasphere model. In R. W. Schunk (Ed.), *Solar-terrestrial energy program: Handbook of ionospheric models, Utah state univ., logan* (pp. 173–206). Utah: Center for Atmospheric and Space Sciences.
- Bailey, G. J., & Sellek, R. (1990). A mathematical model of the Earth's plasmasphere and its application in a study of He^+ at $L = 3$. *Annales de Geophysique*, *8*, 171–189.
- Bailey, G. J., Sellek, R., & Rippeth, Y. (1993). A modelling study of the equatorial topside ionosphere. *Annales de Geophysique*, *11*(4), 263–272.
- Balan, N., & Bailey, G. J. (1995). Equatorial plasma fountain and its effects: Possibility of an additional layer. *Journal of Geophysical Research*, *100*(A11), 21421–21432. <https://doi.org/10.1029/95JA01555>
- Balan, N., Bailey, G. J., Abdu, M. A., Oyama, K. I., Richards, P. G., Macdougall, J., & Batista, I. S. (1997). Equatorial plasma fountain and its effects over three locations: Evidence for an additional layer, the F_3 layer. *Journal of Geophysical Research*, *102*(A2), 2047–2056. <https://doi.org/10.1029/95JA02639>
- Balan, N., Otsuka, Y., Nishioka, M., Liu, J. Y., & Bailey, G. J. (2013). Physical mechanisms of the ionospheric storms at equatorial and higher latitudes during the recovery phase of geomagnetic storms. *Journal of Geophysical Research: Space Physics*, *118*, 2660–2669. <https://doi.org/10.1002/jgra.50275>
- Balan, N., Shiokawa, K., Otsuka, Y., Kikuchi, T., Vijaya Lekshmi, D., Kawamura, S., ... Bailey, G. J. (2010). A physical mechanism of positive ionospheric storms at low latitudes and midlatitudes. *Journal of Geophysical Research*, *115*, A02304. <https://doi.org/10.1029/2009JA014515>
- Balan, N., Shiokawa, K., Otsuka, Y., Watanabe, S., & Bailey, G. J. (2009). Super plasma fountain and equatorial ionization anomaly during penetration electric field. *Journal of Geophysical Research*, *114*, A03310. <https://doi.org/10.1029/2008JA013768>
- Batista, I. S., Abdu, M. A., Souza, J. R., Bertoni, F., Matsuoka, M. T., Camargo, P. O., & Bailey, G. J. (2006). Unusual early morning development of the equatorial anomaly in the Brazilian sector during the Halloween magnetic storm. *Journal of Geophysical Research*, *111*, A05307. <https://doi.org/10.1029/2005JA011428>
- Batista, I. S., de Paula, E. R., Abdu, M. A., Trivedi, N. B., & Greenspan, M. E. (1991). Ionospheric effects of the March 13, 1989, magnetic storm at low and equatorial latitudes. *Journal of Geophysical Research*, *96*(A8), 13,943–13,952. <https://doi.org/10.1029/91JA01263>
- Bittencourt, J. A., & Abdu, M. A. (1981). A theoretical comparison between apparent and real vertical ionization drift velocities in the equatorial F region. *Journal of Geophysical Research*, *86*(A4), 2451–2454. <https://doi.org/10.1029/JA086iA04p02451>
- Blanc, M., & Richmond, A. (1980). The ionospheric disturbance dynamo. *Journal of Geophysical Research*, *85*(A4), 1669–1686. <https://doi.org/10.1029/JA085iA04p01669>
- Burke, W. J., Gentile, L. C., & Huang, C. Y. (2007). Penetration electric fields driving main phase Dst . *Journal of Geophysical Research*, *112*, A07208. <https://doi.org/10.1029/2006JA012137>
- Chau, J. L., & Woodman, R. F. (2004). Daytime vertical and zonal velocities from 150-km echoes: Their relevance to F -region dynamics. *Geophysical Research Letters*, *31*, L17801. <https://doi.org/10.1029/2004GL020800>
- Denardini, C. M., Aveiro, H. C., Almeida, P. D. S. C., Resende, L. C. A., Guizzelli, L. M., Moro, J., ... Abdu, M. A. (2011). Daytime efficiency and characteristic time scale of interplanetary electric fields penetration to equatorial latitude ionosphere. *Journal of Atmospheric and Solar-Terrestrial Physics*, *73*, 1555–1559. <https://doi.org/10.1016/j.jastp.2010.09.003>
- Echer, E., Gonzalez, W. D., & Tsurutani, B. T. (2008). Interplanetary conditions leading to superintense geomagnetic storms ($Dst \leq -250$ nT) during solar cycle 23. *Geophysical Research Letters*, *35*, L06S03. <https://doi.org/10.1029/2007GL031755>
- Fang, X., Liemohn, M. W., Kozyra, J. U., & Evans, D. S. (2007). Global 30–240 keV proton precipitation in the 17–18 April 2002 geomagnetic storms: 2. Conductances and beam spreading. *Journal of Geophysical Research*, *112*, A05302. <https://doi.org/10.1029/2006JA012113>

- Fejer, B. G., Jensen, J. W., Kikuchi, T., Abdu, M. A., & Chau, J. L. (2007). Equatorial ionospheric electric fields during the November 2004 magnetic storm. *Journal of Geophysical Research*, *112*, A10304. <https://doi.org/10.1029/2007JA012376>
- Fejer, B. G., Jensen, J. W., & Su, S.-Y. (2008). Quiet time equatorial *F* region vertical plasma drift model derived from ROCSAT-1 observations. *Journal of Geophysical Research*, *113*, A05304. <https://doi.org/10.1029/2007JA012801>
- Fejer, B. G., & Scherliess, L. (1997). Empirical models of storm time equatorial zonal electric fields. *Journal of Geophysical Research*, *102*(A11), 24,047–24,056. <https://doi.org/10.1029/97JA02164>
- Fuller-Rowell, T., Codrescu, M., Maruyama, N., Fredrizzi, M., Araujo-Pradere, E., Sazykin, S., & Bust, G. (2007). Observed and modeled thermosphere and ionosphere response to superstorms. *Radio Science*, *42*, RS4590. <https://doi.org/10.1029/2005RS003392>
- Fuller-Rowell, T. J., Codrescu, M. V., Rishbeth, H., Moffett, R. J., & Quegan, S. (1996). On the seasonal response of the thermosphere and ionosphere to geomagnetic storms. *Journal of Geophysical Research*, *101*(A2), 2343–2353. <https://doi.org/10.1029/95JA01614>
- Fuller-Rowell, T. M., Millward, G. H., Richmond, A. D., & Codrescu, M. V. (2002). Storm-time changes in the upper atmosphere at low latitudes. *Journal of Atmospheric and Solar - Terrestrial Physics*, *64*(12), 1383–1391. [https://doi.org/10.1016/S1364-6826\(02\)00101-3](https://doi.org/10.1016/S1364-6826(02)00101-3)
- Goncharenko, L. P., Salah, J. E., van Eyken, A., Howells, V., Thayer, J. P., Taran, V. I., ... Chau, J. (2005). Observations of the April 2002 geomagnetic storm by the global network of incoherent scatter radars. *Annales de Geophysique*, *23*, 163–181. <https://doi.org/10.5194/angeo-23-163-2005>
- Hedin, A. E., Fleming, E. L., Manson, A. H., Schmidlin, F. J., Avery, S. K., Clark, R. R., ... Vincent, R. A. (1996). Empirical wind model for the upper, middle and lower atmosphere. *Journal of Atmospheric and Terrestrial Physics*, *58*, 1421–1447. [https://doi.org/10.1016/0021-9169\(95\)00122-0](https://doi.org/10.1016/0021-9169(95)00122-0)
- Huang, C.-S., Rich, R. J., & Burke, W. J. (2010). Storm time electric fields in the equatorial ionosphere observed near the dusk meridian. *Journal of Geophysical Research*, *115*, A08313. <https://doi.org/10.1029/2009JA015150>
- Huang, C.-S., Sazykin, S., Chau, J., Maruyama, N., & Kelley, M. (2007). Penetration electric fields: Efficiency and characteristic time scale. *Journal of Atmospheric and Solar-Terrestrial Physics*, *69*, 1135–1146. <https://doi.org/10.1016/j.jastp.2006.08.016>
- Huba, J. D., Joyce, G., & Fedder, J. A. (2000). Sami2 is Another Model of the Ionosphere (SAM2): A new low-latitude ionosphere model. *Journal of Geophysical Research*, *105*(A10), 23,035–23,053. <https://doi.org/10.1029/2000JA000035>
- Joshi, L. M., Sripathi, S., & Singh, R. (2016). Simulation of low-latitude ionospheric response to 2015 St. Patrick's Day super geomagnetic storm using ionosonde-derived PRE vertical drifts over Indian region. *Journal of Geophysical Research: Space Physics*, *121*, 2489–2502. <https://doi.org/10.1002/2015JA021512>
- Kelley, M. C. (2009). *The earth's ionosphere: Plasma physics & electrodynamics*. San Diego, CA: Academic Press.
- Kelley, M. C., & Dao, E. (2009). On the local time dependence of the penetration of solar wind-induced electric fields to the magnetic equator. *Annales de Geophysique*, *27*, 3027–3030. <https://doi.org/10.5194/angeo-27-3027-2009>
- Kelley, M. C., Makela, J. J., Chau, J. L., & Nicolls, M. J. (2003). Penetration of the solar wind electric field into the magnetosphere/ionosphere system. *Geophysical Research Letters*, *1158*, 2003. <https://doi.org/10.1029/2002GL016321>
- Kelley, M. C., & Retterer, J. (2008). First successful prediction of a convective equatorial ionospheric storm using solar wind parameters. *Space Weather*, *6*, S08003. <https://doi.org/10.1029/2007SW000381>
- Kudeki, E., Bhattacharyya, S., & Woodman, R. F. (1999). A new approach in incoherent scatter *F* region $E \times B$ drift measurements at Jicamarca. *Journal of Geophysical Research*, *104*, 28,145–28,162. <https://doi.org/10.1029/1998JA900110>
- Lin, C. H., Richmond, A. D., Bailey, G. J., Liu, J. Y., Lu, G., & Heelis, R. A. (2009). Neutral wind effect in producing a storm time ionospheric additional layer in the equatorial ionization anomaly region. *Journal of Geophysical Research*, *114*, A09306. <https://doi.org/10.1029/2009JA014050>
- Lin, C. H., Richmond, A. D., Heelis, R. A., Bailey, G. J., Lu, G., Liu, J. Y., ... Su, S.-Y. (2005). Theoretical study of the low- and midlatitude ionospheric electron density enhancement during the October 2003 superstorm: Relative importance of the neutral wind and the electric field. *Journal of Geophysical Research*, *110*, A12312. <https://doi.org/10.1029/2005JA011304>
- Lin, C. H., Richmond, A. D., Liu, J. Y., Bailey, G. J., & Reinisch, B. W. (2009). Theoretical study of new plasma structures in the low-latitude ionosphere during a major magnetic storm. *Journal of Geophysical Research*, *114*, A05303. <https://doi.org/10.1029/2008JA013951>
- Lu, G., Goncharenko, L., Nicolls, M. J., Maute, A., Coster, A., & Paxton, L. J. (2012). Ionospheric and thermospheric variations associated with prompt penetration electric fields. *Journal of Geophysical Research*, *117*, A08312. <https://doi.org/10.1029/2012JA017769>
- Maruyama, N., Richmond, A. D., Fuller-Rowell, T. J., Codrescu, M. V., Sazykin, S., Toffoletto, F. R., ... Millward, G. H. (2005). Interaction between direct penetration and disturbance dynamo electric fields in the storm-time equatorial ionosphere. *Geophysical Research Letters*, *32*, L17105. <https://doi.org/10.1029/2005GL023763>
- Maruyama, N., Sazykin, S., Spiro, R. W., Anderson, D., Anghel, A., Wolf, R. A., ... Millward, G. H. (2007). Modeling storm-time electrodynamics of the low-latitude ionosphere-thermosphere system: Can long lasting disturbance electric fields be accounted for? *Journal of Atmospheric and Solar-Terrestrial Physics*, *69*, 1182–1199. <https://doi.org/10.1016/j.jastp.2006.08.020>
- Panasenko, S. V., & Chernogor, L. F. (2007). Event of the November 7–10, 2004, magnetic storm in the lower ionosphere. *Geomagnetism and Aeronomy*, *47*(5), 608–620. <https://doi.org/10.1134/S0016793207050106>
- Picone, J. M., Hedin, A. E., Drob, D. P., & Aikin, A. C. (2002). NRLMSISE-00 empirical model of the atmosphere: Statistical comparisons and scientific issues. *Journal of Geophysical Research*, *107*(A12), 1468. <https://doi.org/10.1029/2002JA009430>
- Pincheira, X. T., Abdu, M. A., Batista, I. S., & Richards, P. G. (2002). An investigation of ionospheric responses, and disturbance thermospheric winds, during magnetic storms over South America sector. *Journal of Geophysical Research*, *107*(A11), 1379. <https://doi.org/10.1029/2001JA000263>
- Prols, G. W. (1977). Seasonal variations of atmospheric-ionospheric disturbances. *Journal of Geophysical Research*, *82*(10), 1635–1640. <https://doi.org/10.1029/JA082i010p01635>
- Prols, G. W., & von Zahn, U. (1974). Esro 4 Gas Analyzer results 2. Direct measurements of changes in the neutral composition during an ionospheric storm. *Journal of Geophysical Research*, *79*(16), 2535–2539. <https://doi.org/10.1029/JA079i016p02535>
- Retterer, J. M., & Kelley, M. C. (2010). Solar wind drivers for low-latitude ionosphere models during geomagnetic storms. *Journal of Atmospheric and Solar-Terrestrial Physics*, *72*, 344–349. <https://doi.org/10.1016/j.jastp.2009.07.003>
- Richards, P. G., Fennelly, J. A., & Torr, D. G. (1994). EUVAC: A solar EUV flux model for aeronomic calculations. *Journal of Geophysical Research*, *99*(A5), 8981–8992. <https://doi.org/10.1029/94JA00518>
- Richmond, A. D., Peymirat, C., & Roble, R. G. (2003). Long-lasting disturbances in the equatorial ionospheric electric field simulated with a coupled magnetosphere-ionosphere-thermosphere model. *Journal of Geophysical Research*, *108*, 1118. <https://doi.org/10.1029/2002JA009758>
- Rishbeth, H. (1975). *F*-region storms and thermospheric circulation. *Journal of Atmospheric and Terrestrial Physics*, *37*, 1055–1064. [https://doi.org/10.1016/0021-9169\(75\)90013-6](https://doi.org/10.1016/0021-9169(75)90013-6)

- Santos, A. M., Abdu, M. A., Souza, J. R., Sobral, J. H. A., & Batista, I. S. (2016). Disturbance zonal and vertical plasma drifts in the Peruvian sector during solar minimum phases. *Journal of Geophysical Research: Space Physics*, *121*, 2503–2521. <https://doi.org/10.1002/2015JA022146>
- Scherliess, L., & Fejer, B. G. (1999). Radar and satellite global equatorial *F* region vertical drift model. *Journal of Geophysical Research*, *104*(A4), 6829–6842. <https://doi.org/10.1029/1999JA900025>
- Souza, J., Brum, C., Abdu, M., Batista, I., Asevedo, W., Bailey, G., & Bittencourt, J. (2010). Parameterized Regional Ionospheric Model and a comparison of its results with experimental data and IRI representations. *Advances in Space Research*, *46*, 1032–1038. <https://doi.org/10.1016/j.asr.2009.11.025>
- Souza, J. R., Asevedo, W. D. Jr., dos Santos, P. C. P., Petry, A., Bailey, G. J., Batista, I. S., & Abdu, M. A. (2013). Longitudinal variation of the equatorial ionosphere: Modeling and experimental results. *Advances in Space Research*, *51*, 654–660. <https://doi.org/10.1016/j.asr.2012.01.023>
- Taeusch, D. R., Carignan, G. R., & Reber, C. A. (1971). Neutral composition variation above 400 kilometers during a magnetic storm. *Journal of Geophysical Research*, *76*(34), 8318–8325. <https://doi.org/10.1029/JA076i034p08318>
- Tobiska, W., Woods, T., Eparvier, F., Viereck, R., Floyd, L., Bouwer, D., ... White, O. (2000). The SOLAR2000 empirical solar irradiance model and forecast tool. *Journal of Atmospheric and Solar-Terrestrial Physics*, *62*(14), 1233–1250. [https://doi.org/10.1016/S1364-6826\(00\)00070-5](https://doi.org/10.1016/S1364-6826(00)00070-5)
- Torres Pincheira, X. A. (1998). *Resposta do sistema ionosférico-termosférico a tempestades magnéticas no setor Sul-Americano*. Thesis (Doutorado em Geofísica Espacial) - Instituto Nacional de Pesquisas Espaciais (INPE), (INPE-6743-TDI/633) (189 p.), Sao Jose dos Campos. Retrieved from: <http://urlib.net/sid.inpe.br/iris@1905/2005/07.30.05.50>
- Wei, Y., Hong, M., Wan, W., Du, A., Lei, J., Zhao, B., ... Yue, X. (2008). Unusually long lasting multiple penetration of interplanetary electric field to equatorial ionosphere under oscillating IMF B_z . *Geophysical Research Letters*, *35*, L02102. <https://doi.org/10.1029/2007GL032305>
- Wolf, R. A., Sazykin, S., Xing, X., Spiro, R. W., Toffoletto, F. R., de Zeeuw, D. L., ... Goldstein, J. (2013). Direct effects of the IMF on the inner magnetosphere. In J. Burch, M. Schulz, & H. Spence (Eds.), *Inner magnetosphere interactions: New perspectives from imaging* (pp. 127–139). Washington, DC: American Geophysical Union.